Crystalline materials for quantum computing: Semiconductor heterostructures and topological insulators exemplars

High-purity crystalline solid-state materials play an essential role in various technologies for quantum information processing, from qubits based on spins to topological states. New and improved crystalline materials emerge each year and continue to drive new results in experimental quantum science. This article summarizes the opportunities for a selected class of crystalline materials for qubit technologies based on spins and topological states and the challenges associated with their fabrication. We start by describing semiconductor heterostructures for spin qubits in gate-defined quantum dots and benchmark GaAs, Si, and Ge, the three platforms that demonstrated two-qubit logic. We then examine novel topologically nontrivial materials and structures that might be incorporated into superconducting devices to create topological qubits. We review topological insulator thin films and move onto topological crystalline materials, such as PbSnTe, and its integration with Josephson junctions. We discuss advances in novel and specialized fabrication and characterization techniques to enable these. We conclude by identifying the most promising directions where advances in these material systems will enable progress in qubit technology.

Introduction

The quality of solid-state qubit platforms such as spin qubits, superconducting qubits, or topological qubits, strongly depends on the quality of the host material for their performance.

Unfortunately, most existing solid-state qubits suffer from significant decoherence caused by a variety of material challenges, including point defects, grain boundaries, and interface contamination. Improving the quality of materials and heterostructures was of fundamental importance for the creation of classical transistors found in modern computers. Improving the quality of the quantum materials housing solid-state qubits is likely to play a similarly crucial role in the development of quantum computers.

One of the major breakthroughs in the synthesis of GaAs-based heterostructures for solid-state electronics and optoelectronics was the use of molecular beam epitaxy (MBE). MBE is an ultrahigh vacuum technique in which thin films are grown one layer of atoms at a time. Elements are thermally evaporated from effusion cells and travel to a heated substrate as molecular beams. When the atoms reach the substrate, they bond to the substrate and to each other, forming one atomic layer with an epitaxial relationship to the substrate. The film is then grown one layer of atoms at a time. MBE can easily be used to grow thin films with precise composition, thickness, and doping density. In addition, different materials with similar lattice constants can be stacked together to form complex heterostructures. Finally, strain-driven self-assembly can be used to form quantum dots, nanowires, or other quantum-confined structures embedded within or on top of other materials. MBE is now widely used in both research labs and in industry to grow a huge variety of materials, including semiconductors, oxides, chalcogenides, and metals.

G. Scappucci, QuTech and Kavli Institute of Nanoscience, Delft University of Technology, The Netherlands; g.scappucci@tudelft.nl
P.J. Taylor, US Army Research Laboratory, USA; patrick.j.taylor36.civ@mail.mil
J.R. Williams, Department of Physics, University of Maryland, USA; jrwill@umd.edu
T. Ginley, National Institute of Standards and Technology, USA; theresa.ginley@nist.gov
S. Law, Department of Materials Science and Engineering and Department of Physics and Astronomy, University of Delaware, USA; slaw@udel.edu
*Corresponding author

doi:10.1557/s43577-021-00147-8

© The Author(s) 2021

Critical advancements in the development of reduced pressure chemical vapor deposition (CVD) industrial tools have made it possible to grow high-volume Group-IV heterostructures also in academic settings. In CVD, molecules from growth precursor gases (e.g., SiH_4 and GeH_4) land on a heated substrate surface. The molecules partly decompose, hydrogen desorbs, and Si or Ge atoms form an epitaxial layer. By using an industrial manufacturing compatible process, near-perfect deposition of Si, Ge, and SiGe layers is achieved with precise control over layer thicknesses, strain, and with very low background of impurities and defects. The proven quality of these "quantum ready" Si/Ge materials stacks has already enabled rudimentary quantum algorithms on spin–qubit processors.

The power of MBE, CVD, and related epitaxial techniques, to grow new materials and heterostructures can be harnessed to advance progress in quantum materials and devices, as we describe in this article.

Semiconductor heterostructures

Overview

Semiconductor heterostructures find widespread use in solid-state quantum computing platforms, ranging from quantum-dot spin–qubits processors, to qubit proposals based on topological insulators. To illustrate some of the opportunities and challenges associated with semiconductor heterostructures, we focus on spin qubits in gate-defined semiconductor quantum dots.[1] Quantum-dot spin qubits are a promising platform for large-scale integration of quantum components, due to the striking resemblance of quantum-dot devices to classical transistors,[2,3] which are integrated by the billions into a single chip. To host spin qubits in gate-defined quantum dots, a single electron or hole is trapped in the potential landscape obtained by a combination of heterogeneous materials, interfaces, and gate electrodes.[4,5] Here, we focus on GaAs, Si, and Ge, three semiconductor platforms that have demonstrated the key functionality of two-qubit quantum logic.[6–8] In **Figure 1**, the platforms are qualitatively compared by considering materials stacks and quantum-dot architectures. In the following, we discuss additional relevant heterostructure benchmarks, their integration aspects and two electrical transport metrics—mobility and percolation density—that serve as useful qualifiers for disorder due to materials and gate stacks. Maximum mobility (μ) is a popular metric to gauge the disorder potential landscape in the material. However, mobility peaks at high carrier density due to screening—not the regime of operation for quantum-dot qubits. The percolation density (n_p) is an additional metric to characterize disorder relevant for quantum dots, since it measures the minimum density required to establish metallic conduction by overcoming charge trapping in the disorder potential landscape.

Gallium arsenide

Spin qubits in gate-defined quantum dots were first demonstrated in GaAs[4,9] due to favorable band structure properties and the maturity of MBE growth of heterostructures based on III–V compounds. In a typical modulation-doped GaAs/AlGaAs heterostructure the conduction-band offset at the GaAs/AlGas interface supports a two-dimensional electron gas (2DEG), populated from a nearby Si-doped AlGaAs layer. GaAs and AlGaAs are nearly lattice-matched, so GaAs/AlGas heterostructures have an exceptional structural quality, allowing for large electron mobility (10^6–10^7 cm^2) and low percolation density ($<10^{10}$ cm^{-2}/Vs).[10] Consequently, quantum dots of about $1/\sqrt{n_p}$= 100 nm in size, informative about the average distance between traps, are essentially disorder-free.

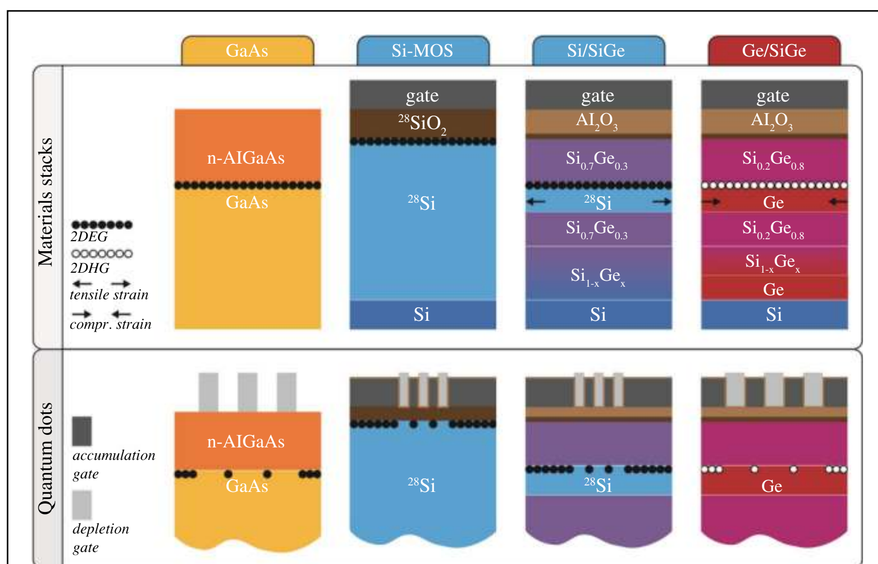

Figure 1. GaAs, Si, and Ge semiconductor materials for quantum-dot spin qubits. The top and bottom row compare materials stacks and quantum-dot architectures for GaAs, Si-MOS, Si/SiGe, and Ge/SiGe (left to right columns). In quantum wells (GaAs, Si/SiGe, and Ge/SiGe) disorder is low compared to Si-MOS due to the separation of the conducting channel from scattering charge at the surface. In GaAs, the quantum well is typically 50–80 nm below the surface. In Si/SiGe and Ge/SiGe the distance from the quantum well to the dielectric interface is typically 30–60 nm. Ge quantum wells are thicker (≈16 nm) than Si quantum wells (≈10 nm). In quantum dots, the accumulation gate pitch is tighter in Si (≈ 80 nm) than in Ge[19] due to the heavier effective mass (0.19m_e in Si versus 0.05m_e in Ge).

To define quantum dots, the 2DEG is locally depleted by Schottky gates. The absence of dielectrics preserves the low disorder of the pristine heterostructure and increases device yield. The single conduction-band valley and low

effective mass ($m^* = 0.067m_e$) enable quantum dots that have large energy spacings and are relatively easy to fabricate. The sizable spin–orbit interaction allows for local all-electrical manipulation of single spins.[11] The main drawback of GaAs is the hyperfine coupling to the nuclear spin bath, causing severe qubit decoherence.[12] Furthermore, the challenging integration of GaAs on a Si wafer limits the prospect of integrating large numbers of qubits into a practical quantum processor.

Silicon

The two main limitations of GaAs become the main drivers to pursue spin qubits in Si. The most common isotope, ^{28}Si, has zero nuclear spin, significantly reducing hyperfine-induced dephasing, providing long quantum coherence.[1,3,5,13] Furthermore, there is the promise to leverage advanced semiconductor manufacturing for the integration of qubits in the large numbers required for fault-tolerant quantum computing. Spin qubits in Si are implemented in metal oxide semiconductor (Si-MOS) structures or in Si/SiGe heterostructures. In Si-MOS, a 2DEG is confined at the interface between Si and SiO_2, both of which can be isotopically purified. Multiple layers of gates, insulated by dielectrics, accumulate and confine charge into quantum dots.[14] These gates have a rather tight pitch because of the large effective mass ($0.19m_e$), requiring quantum dots in Si to be much smaller than in GaAs. Following the availability of $^{28}SiH_4$ gas for ^{28}Si deposition,[15,16] isotopically purified Si-MOS spin qubits were fabricated in a 300-mm semiconductor manufacturing facility using all-optical lithography and fully industrial processing.[17] In these qubits, Si finFETs[18] provide conducting channels, and gates on top define quantum dots along the fin.

The presence of multiple conduction bands is a limitation of Si,[5] because the small energy separation (valley splitting) between the ground state and the lowest excited state complicates quantum operations. However, due to the strong confinement at the sharp semiconductor/oxide interface, valley splitting in Si-MOS can be substantial[20] (up to 1 meV), making it possible to operate Si qubits at "hot" temperatures of 1 K.[21] This is encouraging for cointegration of CMOS-based cryogenic control circuits and silicon quantum processors.[22]

The main drawback of Si-MOS is the proximity of the qubit to the very disordered oxide interface. Mobility is rather low ($\approx 10^4$ cm^2/Vs at best[15,23,24]) and the percolation density high ($\approx 10^{11}$ cm^{-2}).[15] Because low disorder is especially important for multi-quantum-dot systems, this remains an important consideration.

Disorder is greatly mitigated in Si/SiGe heterostructures, because the 2DEG is accumulated at the buried interface between a Si quantum well under tensile strain and a $Si_{1-x}Ge_x$barrier (Ge concentration $x \approx 0.3$).[25] Similar Si-MOS, the Si quantum well can be isotopically enriched to ^{28}Si for long quantum coherence.[26] Differently than GaAs, Si/SiGe heterostructures for quantum-dot spin qubits are undoped,[27] and electrons populate the quantum well via voltages applied to top gates. High-quality Si/SiGe poses additional challenges compared to GaAs/AlGaAs because of the 4.2% lattice mismatch between Si and Ge. The Si quantum well is deposited on a strain-relaxed SiGe buffer obtained by gradually increasing the Ge concentration in the SiGe alloy to accommodate the lattice mismatch between Si and Ge. After decades of advancements, Si/SiGe heterostructures, grown by industrial reduced pressure chemical vapor deposition (RP-CVD), are a rather mature platform with high mobility ($\approx 10^5$ cm^2/Vs) and low percolation density ($\approx 10^{10}$ cm^{-2}),[28–30] expected to further improve by leveraging advanced semiconductor manufacturing processes for optimizing the gate stack. Fabrication of quantum dots in Si/SiGe relies on overlapping gate structures for tightly spaced quantum dots with gate-tunable tunnel barriers. Due to the low disorder, device yield is high, making it possible to define and control large linear arrays of quantum dots.[31]

The current major challenge with Si/SiGe is the lower valley splitting (50 to 200 μeV),[32–35] compared to Si-MOS, due to the atomistic imperfection and chemical disorder at the epitaxial Si/SiGe interface. However, first steps are being taken to improve the heterostructures by incorporating more complex Ge concentration profiles[36] for increased the valley splitting.

Germanium

While most studies have focused on electrons, holes in strained Ge/SiGe heterostructures have recently emerged as a compelling platform that offers low disorder, all-electrical qubit control, and avenues for scaling.[37] Ge combines many advantages of Si and GaAs while overcoming most of their limitations. Ge is a CMOS-foundry material and can be isotopically engineered for long quantum coherence. The high mobility, low effective mass, and sizable spin–orbit coupling imply large energy spacing for easy fabrication of quantum dots with full electrical qubit control.

In a typical Ge/SiGe heterostructure[38] holes are confined at the interface between a compressively strained Ge quantum well and a $Si_{1-x}Ge_x$barrier ($x \approx 0.8$). Strain and size quantization remove the valence-band degeneracy, so holes in Ge/SiGe are a single-band system, overcoming the main limitation of electrons in Si. Starting from a Si wafer, a strain-relaxed Ge layer is grown, followed by a graded $Si_{1-x}Ge_x$layer in which the Ge concentration is progressively reduced to ≈ 0.8 (reverse grading). The strain-relaxed SiGe buffer serves as a virtual substrate for the coherent deposition of the Ge quantum well, the SiGe barrier, and a final sacrificial Si cap. Modulation doping is avoided and charge carriers populate the quantum well via voltages applied to top gates. Optimized Ge/SiGe stacks are grown by RP-CVD and have similar levels of disorder as Si/SiGe, with $\mu \approx 10^5$ cm^2/Vs[38] and $n_p \approx 10^{10}$ cm^{-2}.[39]

Quantum-dot qubits[8] are defined by a set of multilayer gates, with a less stringent pitch than in Si, due to the light effective mass ($0.05m_e$).[40] The low disorder in Ge/SiGe has allowed for the rapid progress in only two years from single quantum dots[41] to a four-qubit system[42] with controllable

coupling along both directions in a 2 × 2 array, setting the benchmark for spin–qubit quantum processors.

Topological insulators

Overview

One of the major hurdles to advancing quantum computing is qubit decoherence. The short decoherence times associated with solid-state qubits mean that all computing operations must take place faster than the qubit decoheres, which is extremely challenging. Topological materials may provide a route to creating topologically protected qubits where coherence times may be greatly enhanced. Topological insulators that possess superconducting correlations—called topological superconductors—are predicted to host Majorana bound states (MBS), which can be used as a basis for topological quantum computation.

The class of topologically nontrivial materials that can serve as a platform for MBS includes topological insulators (TIs), Dirac semimetals (DSMs), and Weyl semimetals (WSMs). For a detailed discussion of these material classes, see References 43 and 44. These materials are distinguished from normal materials by the topology of their band structure. In a normal material, the wave function of the conduction-band electrons will have a particular symmetry throughout the Brillouin zone (e.g., *s*-symmetry), while the valence band will have a different symmetry (e.g., *p*-symmetry). In a topological material, the symmetry of the valence- and conduction-band states can be reversed at particular points within the Brillouin zone. For example, at the Γ point, the conduction-band states may have *p*-symmetry, while the valence-band states may have *s*-symmetry. This type of band inversion frequently arises in materials with large spin–orbit coupling, which is why topological materials usually include one or more heavy elements. When a topological material comes into contact with a normal material, this band inversion needs to "unwind," resulting in the formation of topologically protected surface states.

TIs always preserve time-reversal symmetry. They usually have a band structure comprising a bulk bandgap with topologically protected surface states crossing the bandgap at the Γ point. These surface states are linearly dispersing, two-dimensional, and exhibit spin-momentum locking. Particles occupying these surface states therefore have a high Fermi velocity and limited scattering paths into other surface states as a change in momentum requires a change in spin. On the other hand, WSMs exhibit either broken inversion symmetry or broken time-reversal symmetry. In the simplest incarnation of the WSM, this symmetry-breaking results in two symmetric points in the band structure where the conduction and valence bands touch and exhibit linear dispersion. These two points have opposite chirality and always appear in pairs. A point of positive chirality is a source of Berry curvature, while a point of negative chirality is a sink of Berry curvature. One of the key signatures of a WSM is the existence of surface Fermi arcs at the interface between a WSM and a normal material, similar to the surface states that arise at a TI/normal material interface. These Fermi arcs will always connect the two Weyl points of opposite chirality. The separation of the two Weyl points in momentum space is related to the strength of the symmetry-breaking perturbation. As the strength of this perturbation is reduced, the Weyl points move closer together. Eventually, they merge, forming a transitional state before returning to a normal insulator. WSMs can have more than two Weyl nodes, and those nodes can have complex Fermi surfaces. Finally, the DSM state is a special case of the WSM in which both time-reversal and inversion symmetry are present. In this case, Weyl nodes that are degenerate in energy but with opposite chirality can exist at the same point in momentum space. This state can generally be gapped out by small perturbations, but it can be stabilized in materials that show specific space group symmetries or with the application of strain to a TI.

In addition to time-reversal symmetry-protected topological materials, the point group symmetry of the crystal lattice can also provide a path to topological phases of matter. These topological insulators are called topological crystalline insulators (TCIs). Their band structure is similar to the topological insulators discussed earlier, but the band inversion is caused by the symmetry of the lattice rather than strong spin–orbit coupling. This not only greatly expands the number of materials capable of being topological, but offers important technological advantages that are important in moving the field forward for quantum computation. Spatial symmetries, strain and defects can be tailored during growth, each playing an important role in determining the electronic properties of the surface state. Experimental knobs—such as electric fields—can be engineered into device designs to allow for in situ tunability of the topology, allowing for enhanced state control and alleviating variability between individual qubits. A review of the theoretical aspects of topological crystalline insulators can be found in Reference 45.

The theoretical aspects of topological materials lie on a solid foundation, leaving the frontier of the field to condensed-matter experimentalists and materials scientists. A main challenge for condensed-matter experimentalists is in characterization of topological phases of matter: concrete determination of the topological state will likely involve moving beyond conventional characterization techniques such that the topological state can ascertained with precision. For materials scientists, a primary challenge lies in creating more perfect materials and interfaces, which can mitigate imperfections that hide the true nature of the exotic excitations possible in the system. Along these two fronts, a process for creating a more perfect material using MBE and using superconducting nanoscale devices to characterize the topological nature of the material is described next.

Incorporation of topological materials into superconducting devices not only allows for characterization but serves as means to produce topological superconductors (TSs). TS may play a key role in future quantum computation platforms, as the fundamental excitations of these systems are MBS, a non-Abelian

excitation comprised of equal weights of electron- and hole-like quasiparticles. These excitations can form the foundation for a topological qubit and its incorporation in nanoscale superconducting electronics allows for the generation, manipulation, and readout of these qubits. While a detailed review of topological superconductors and the MBS therein can be found in References 45 and 46, the two key elements that go into the creation of this state are simple. The first is the nondegenerate electronic state at the Fermi energy: this element is provided by the topological materials. The second is a quasiparticle that combines electron and hole-like properties in equal weight. This is provided by the superconductors used to form the nanoscale device. Despite the clear-cut recipe for the creation of MBS, the two challenges elucidated above for topological materials also confront MBS. For the MBS to be used in topological quantum computation, these challenges must be overcome. Next, we describe the progress along these directions for the growth and characterization of both TIs and TCIs.

Molecular beam epitaxy growth of topologically nontrivial thin films

The growth of thin films of topologically nontrivial materials by MBE is a crucial enabling technology to study these materials, as many of their applications rely on the interface between the topological material and the trivial material. Although these materials can be grown by a variety of techniques, we focus on MBE growth here. Since MBE is an ultrahigh vacuum technique in which materials are grown one atomic layer at a time, clean and sharp interfaces between layers can be produced, which are crucial to leveraging the unique properties of topological materials. In addition, MBE enables the growth of large area films out of thermal equilibrium and without the need for complex chemical precursors which can add unwanted dopants to a film. First- and second-generation TIs, including Bi_2Se_3, Bi_2Te_3, Sb_2Te_3, and their alloys are perhaps the most well-studied topological materials. They are van der Waals (vdW) materials, meaning that they are strongly bonded in the $a-b$ plane and have weaker vdW bonds along the c-axis. The growth of vdW materials by MBE is called "van der Waals epitaxy."[47,48] In vdW epitaxy, the film/substrate interaction is much weaker than in traditional epitaxy, allowing for growth on a wide variety of substrates, even those with considerable lattice mismatches.[49] This leeway in substrate choice, combined with the ability to alloy and magnetically dope these materials, has enabled successful film growth for many different applications. A large fraction of TI growth has been conducted on sapphire substrates due to their relatively low cost and inert growth surface. Other substrates may have dangling bonds that must be passivated before growth; a chalcogenide soak is frequently used to accomplish this. This method has been used to facilitate growth on substrates such as GaAs(111),[50] GaAs(001),[51] InP(111)A,[52] and Si(111).[53,54]

One of the challenges with vdW epitaxy is the reduced control over film morphology. TI films tend to grow as triangular domains with a high degree of twinning and a terraced pyramidal morphology. The in-plane unit cell of the TI is hexagonal with three sides that have two dangling bonds per atom and three sides that have one dangling bond per atom. The sides with more dangling bonds grow faster, leading to triangular domains. Twinning in TI films arises since their triangular in-plane structure means that domains can nucleate with two different orientations rotated by 180°. When the twinned domains merge, grain boundaries appear, which cause electron scattering. Growth on rougher substrates can suppress twinning by pinning nucleation along the substrate step edges.[55] Finally, due to the weak vdW bonding between layers, TI films show a terraced or "wedding cake" morphology.[56] This leads to a high density of atomic step edges in the film, increasing scattering. Although the film/substrate interaction is small in vdW epitaxy, many researchers observe a high degree of disorder in the film at the interface with the substrate.[57,58] This can lead to significant doping and is likely the cause of the majority of doping in TI thin films, rather than point defects such as selenium vacancies. Using a trivially insulating lattice-matched buffer layer such as In_2Se_3 or $(In_xBi_{1-x})_2Se_3$ can bury this disordered layer and isolate the TI, reducing doping and increasing mobility.[59,60] $(In_xBi_{1-x})_2Se_3$ is also useful for growing TI heterostructures as it is trivially insulating when $x>0.3$.[61,62] MBE-grown heterostructures have also been used to explore the interaction of magnetic materials with TIs[63] or to create designer TI behavior through ultrashort period lattices,[64] or explore the interactions of the surface states.[65]

The properties of MBE-grown TI films can be customized through both alloying and doping. Alloying Bi_2Te_3 and Sb_2Te_3 has been explored to create bulk insulating TI films and to pull the Dirac point of Bi_2Te_3 into the bandgap.[66] Chalcogenide-based TIs tend to suffer from point defects, including chalcogen vacancies and antisite defects, which lead to unintentional doping.[67] Nonmagnetic dopants such as calcium and lead have been used to tune the Fermi energy,[68,69] while magnetic materials such as vanadium,[70] chromium,[71] and manganese[72] have been studied as dopants to break the time-reversal symmetry of the surface states and allow for easier study of phenomenon such as the quantum anomalous Hall effect in TI thin films. Finally, while most MBE growth of TIs has focused on perfecting smooth, continuous films in the [111] orientation, a growing body of research has begun to examine the growth of alternate phases and self-assembled nanofeatures. Growth of $(10\bar{1}5)$ Bi_2Se_3 has been achieved by patterning the substrate[73] or through growth at high substrate temperature and high selenium overpressure on GaAs (001) substrates.[74] Bi_2Se_3 nanoparticle growth has been demonstrated via exposing bismuth droplets to a selenium flux.[75] More exotic 3D features such as columns and nanoplates have also been reported.[76]

In the past handful of years, there have been many predictions of materials that may be WSMs or DSMs. Only a small subset of these materials have been grown in thin-film form, and those can be divided roughly into two categories: those grown by van der Waals epitaxy, and those grown by more conventional epitaxy. Materials grown by van der Waals

epitaxy include but are not limited to $MoTe_2$, $ZrTe_2$, $PtSe_2$, $PtTe_2$, $HfTe_2$.[77–82] In general, all are grown in a similar way to the TIs previously described: the chalcogenide member is held in excess, while the non-chalcogenide member controls the growth rate. However, for these, materials, the non-chalcogenide member is frequently evaporated using electron beam evaporation rather than thermal evaporation due to the low vapor pressures of the relevant transition metals. Since these materials are grown by vdW epitaxy and have a hexagonal in-plane structure, they have the same advantages and disadvantages described for the TIs. Materials grown by conventional epitaxy include Cd_3As_2, NbP, TaP, Na_3Bi, Sr_3PbO, LaAlGe, $Co_3Sn_2S_2$, and $TaIrTe_4$.[83–91] In most of these cases, the more volatile element (i.e., As, P, S, Te) is held in excess, while the less volatile element controls the growth rate. However, in the cases of materials like LaAlGe or Na_3Bi, more careful flux matching is needed. Finally, because these are grown by conventional epitaxy, one must take care to find a lattice-matched substrate and to prepare the substrate appropriately for the film growth. Overall, it is clear to see that there is a wealth of topological materials that can be grown by MBE. Thin films of topological materials are particularly interesting, as they enable other characterization techniques such as scanning tunneling microscopy and angle resolved photoemission spectroscopy. Overall, the growth of topological materials by MBE is in its infancy, but just as MBE growth of semiconductor materials has led to a wealth of scientific discoveries and device applications, we expect that MBE growth of topological materials will do the same.

Molecular beam epitaxy growth of the TCI $Pb_xSn_{1-x}Te$

The PbSnTe system is a cubic alloy system with large spin–orbit coupling whose energy gap is widely tunable. The topological nature derives from a nonzero mirror Chern number arising from its crystal symmetry. As the as the ratio of Sn to Te is increased, there is a semimetal band crossover with the emergence of two types of Dirac cones on (111): one type at the Γ point and another type at the M point, with an energy offset between them. PbSnTe devices can host 3D massive, or 2D massless relativistic fermions, and by introducing strain, 3D Weyl semimetallic states are possible.[45]

The mesoscale dimensionality of Josephson junctions (JJs), an important method to characterize MBSs, imposes some requirements for the active material forming the weak link, and there are challenging materials issues associated with these requirements. Of particular importance is surface roughness, which can scatter topological surface states into the bulk.[92]

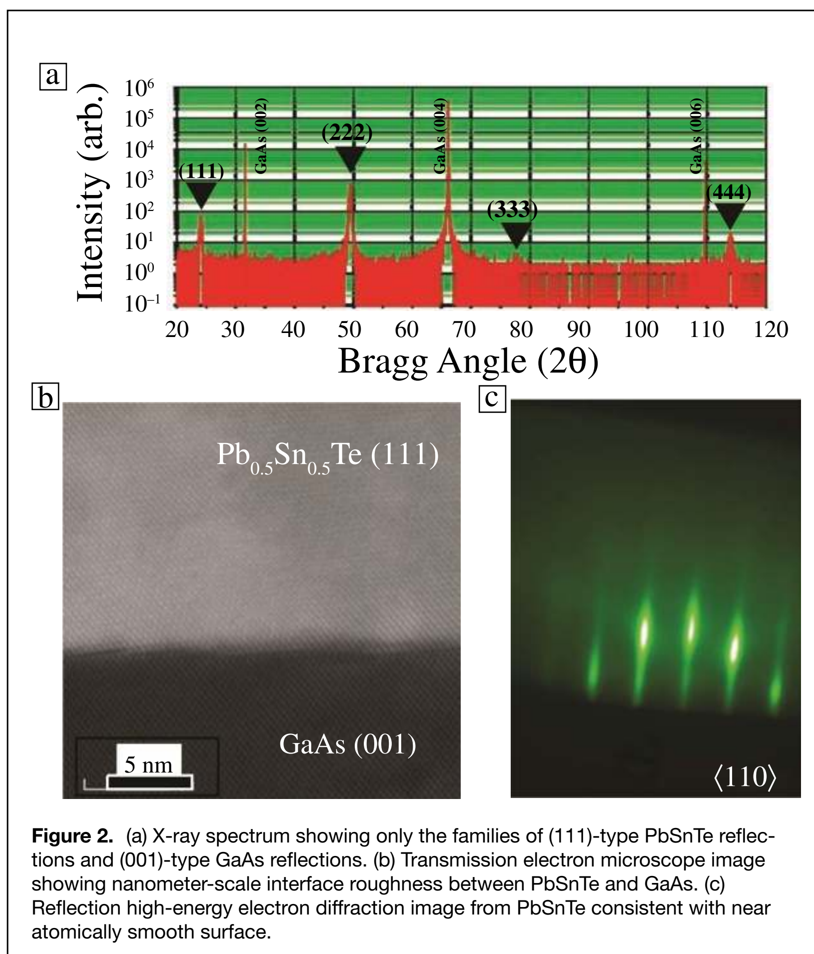

Figure 2. (a) X-ray spectrum showing only the families of (111)-type PbSnTe reflections and (001)-type GaAs reflections. (b) Transmission electron microscope image showing nanometer-scale interface roughness between PbSnTe and GaAs. (c) Reflection high-energy electron diffraction image from PbSnTe consistent with near atomically smooth surface.

To address these issues, a different MBE approach was adopted. Elemental sources of Pb and Sn metals (IV elements), and Te (VI element) were used to obtain single-crystal PbSnTe device layers on GaAs (**Figure 2**). This elemental approach enables better control over the nucleation, and helps reduce undesirable Volmer–Weber island coalescence. Near atomically flat, thin layers are obtained that more effectively localize the topological state to the surfaces. GaAs enables scalability at low cost, and its bulk can be made electrically insulating. While this approach successfully facilitates JJ fabrication, it is not optimized, leaving room for improvement in future growths. One remaining major challenge is the large carrier concentration of PbSnTe bulk states. These bulk states allow for scattering from the surface state and shunt the measured conductance, two effects that minimize the experimental signatures of MBS.

Characterizing the TCI $Pb_xSn_{1-x}Te$ with Josephson junctions

The Josephson effect describes how electric currents of Cooper pairs can flow between two superconductors as the quantum phase difference between

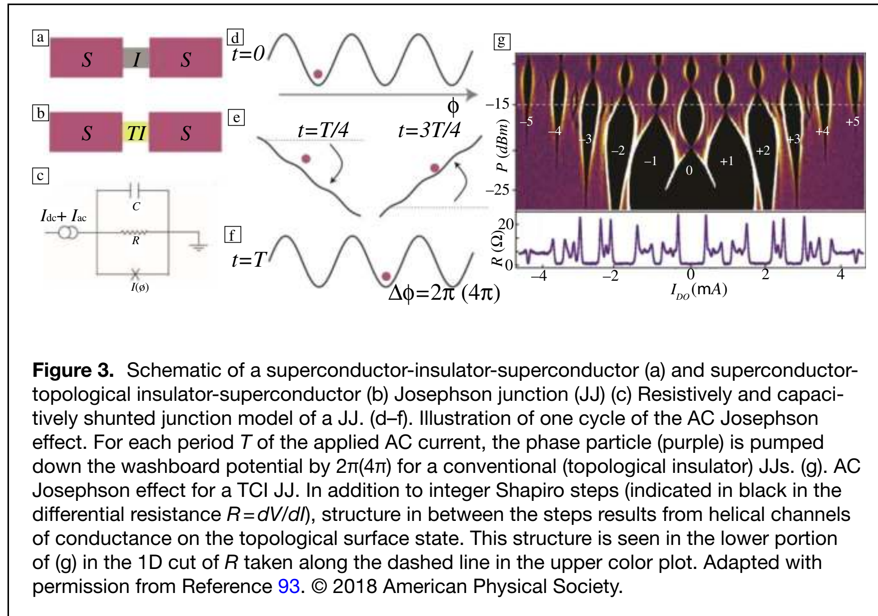

Figure 3. Schematic of a superconductor-insulator-superconductor (a) and superconductor-topological insulator-superconductor (b) Josephson junction (JJ) (c) Resistively and capacitively shunted junction model of a JJ. (d–f). Illustration of one cycle of the AC Josephson effect. For each period T of the applied AC current, the phase particle (purple) is pumped down the washboard potential by $2\pi(4\pi)$ for a conventional (topological insulator) JJs. (g). AC Josephson effect for a TCI JJ. In addition to integer Shapiro steps (indicated in black in the differential resistance $R=dV/dI$), structure in between the steps results from helical channels of conductance on the topological surface state. This structure is seen in the lower portion of (g) in the 1D cut of R taken along the dashed line in the upper color plot. Adapted with permission from Reference 93. © 2018 American Physical Society.

the superconductors is adjusted. Nearly 60 years ago, Brian Josephson predicted this for an ordinary JJ (a superconductor-insulator-superconductor sandwich (**Figure 3**a), finding that the supercurrent I_S was determined by the phase difference φ between the two superconductors is $I_S = I_C\sin\varphi$. I_C is the maximal supercurrent the JJ can sustain before the current begins to be dominated by a normal electronic current. When the insulator is replaced by a conducting weak link (Figure 3b) this relation between the supercurrent and phase, called the current-phase relation (CPR), is altered: in some cases this alteration reveals important properties about the conductor. Weak links made of topological insulators are an example of this. In this case, the CPR changes to $I_S = I_C\sin(\varphi/2)$. The shift in CPR arises from the presence of MBS at the interface of the superconductor and topological insulator.

This change in CPR allows for a binary test for topological materials. A straightforward way to perform this test is the AC Josephson effect. This effect can be understood using a common electric model for a JJ called the resistively and capacitively shunted junction model (RCSJ) (Figure 3c).[94] This model is isomorphic with a particle moving under the influence of a sinusoidal potential (Figure 3d). The AC Josephson effect is explored by rocking this potential up and down with an AC current and pumping the particle along the potential (Figure 3d–f). In this scenario, the junction picks up a voltage that depends on the phase accumulated per pump, producing a series of steps in the $I-V$ curve called Shapiro steps. This accumulated phase is 2π for common conducting weak links, producing a voltage of $hf/2e$ where f is the AC frequency of the applied current and h, e are Planck's constant and the electron charge, respectively. For topological weak link JJs, the accumulated phase is 4π, producing steps exactly twice as large (hf/e) as conventional JJs. Hence, the doubling of phase accumulation indicative of a topological superconducting state and the presence of MBS can be read out as doubled height of the Shapiro steps.[95]

In TCI samples, atomic-scale variations of the crystal lattice at the surface alter the simple picture of a two-dimensional topological surface state. Step edges on the surface cut helical one-dimensional helical channels on the surface,[6] complicating the signature of Majorana bound states. Despite being embedded in other, conventional conduction channels, these one-dimensional helical modes can still be read out using the AC Josephson effect.[93] The reason is that these helical channels have near unity transmission, which "skews" the CPR from sinusoidal to one containing prominent higher harmonics. These higher harmonics produce structure in the Shapiro steps between the primary plateau (Figure 3g), which can be used to read out modifications to the CPR.

Outlook

Despite the immense progress in both the growth and applications of crystalline materials for quantum computing, challenges remain. With regard to semiconductor heterostructures for spin qubits, it is still unclear which material will be powering a large-scale spin–qubit quantum processor. However, the most significant advancements in the field can be traced back to leaps in materials developments. Silicon gained popularity over GaAs because the integration of ^{28}Si enabled long quantum coherence. Germanium has attracted attention since hole spin qubits have progressed at an extraordinary pace. The Ge qubit count has doubled roughly every year and larger systems are on the horizon. The Ge quantum information route[37] is poised to retain many advantages of GaAs and Si while overcoming some of their respective long-standing challenges.

Regardless of the material of choice, increasingly fast feedback cycles are required to accelerate the development of quantum materials. Important steps in this direction have been taken. Cryo-multiplexing technology[30,96] mitigates the interconnect bottleneck present in cryostats operating at mK temperatures. Therefore, we can access with high-throughput the low-temperature quantum transport properties of 2D electrons or holes relevant for spin qubits. Hopefully, high-throughput characterization will also apply to charge noise measurements. Fast optimization of the material and gate stack parameters is essential as we are moving into the next phase of engineering qubit systems in the large numbers required for useful quantum computing.

Since the original theoretical proposal of time-reversal-symmetric topological insulators of the mid 2000s, dramatic progress has been made in cataloging the zoo of topological

states of matter possible in condensed-matter systems. Yet, much work needs to be done in these systems before they can be fully considered for use in quantum computation: in particular in the area of materials quality and characterization. The advances made using MBE to grow thin films of topological materials opens the possibility to address both these challenges. Controlled layer-by-layer growth enables enhanced control over the crystal structure, disorder, surface quality and strain, each of which have important consequences for the valuable topological surface state. Layering of topological and trivial materials can open doors to new device functionality. Further, the ability to control composition will allow for functional interfaces—like the superconductor-TI interface important for the creation of MBS. This technology has already showed promise in both GaAs- and topological material systems. Thin films will also enable new types of experimental devices, which will not only enhance the technological application of TI materials, but should prove useful in augmenting the characterization techniques useful in discerning topological from trivial effects.

Acknowledgments

S.L. acknowledges support from the US Department of Energy, Office of Science, Office of Basic Energy Sciences, under Award No. DE-SC0017801. G.S. acknowledges support from NWO, Netherlands Organization for Scientific Research. P.J.T. and J.R.W. were sponsored by the grants National Science Foundation A “Quantum Leap” Demonstration of Topological Quantum Computing (DMR-1743913), Physics Frontier Center at the Joint Quantum Institute (PHY-1430094), and the Army Research Office Award W911NF-18-2-0075.

Conflict of interest

The authors declare that they have no conflict of interest.

Open Access

This article is licensed under a Creative Commons Attribution 4.0 International License, which permits use, sharing, adaptation, distribution and reproduction in any medium or format, as long as you give appropriate credit to the original author(s) and the source, provide a link to the Creative Commons license, and indicate if changes were made. The images or other third party material in this article are included in the article’s Creative Commons license, unless indicated otherwise in a credit line to the material. If material is not included in the article’s Creative Commons license and your intended use is not permitted by statutory regulation or exceeds the permitted use, you will need to obtain permission directly from the copyright holder. To view a copy of this license, visit http://creativecommons.org/licenses/by/4.0/.

References

1. D. Loss, D.P. DiVincenzo, Quantum computation with quantum dots. *Phys. Rev. A* **57**, 120 (1998)
2. L.M.K. Vandersypen, H. Bluhm, J.S. Clarke, A.S. Dzurak, R. Ishihara, A. Morello, D.J. Reilly, L.R. Schreiber, M. Veldhorst, Interfacing spin qubits in quantum dots and donors—hot, dense, and coherent. *npj Quantum Inf.* **3**(1), 34 (2017)
3. L.M.K. Vandersypen, M.A. Eriksson, Quantum computing with semiconductor spins. *Phys. Today* **72**(8), 38 (2019)
4. R. Hanson, L.P. Kouwenhoven, J.R. Petta, S. Tarucha, L.M.K. Vandersypen, Spins in few-electron quantum dots. *Rev. Mod. Phys.* **79**, 1217 (2007)
5. F.A. Zwanenburg, A.S. Dzurak, A. Morello, M.Y. Simmons, L.C.L. Hollenberg, G. Klimeck, S. Rogge, S.N. Coppersmith, M.A. Eriksson, Silicon quantum electronics. *Rev. Mod. Phys.* **85**, 961 (2013)
6. K.C. Nowack, M. Shafiei, M. Laforest, G.E.D.K. Prawiroatmodjo, L.R. Schreiber, C. Reichl, W. Wegscheider, L.M.K. Vandersypen, Single-shot correlations and two-qubit gate of solid-state spins. *Science* **333**(6047), 1269 (2011)
7. M. Veldhorst, C.H. Yang, J.C.C. Hwang, W. Huang, J.P. Dehollain, J.T. Muhonen, S. Simmons, A. Laucht, F.E. Hudson, K.M. Itoh, A. Morello, A.S. Dzurak, A two-qubit logic gate in silicon. *Nature* **526**(7573), 410 (2015)
8. N. Hendrickx, D. Franke, A. Sammak, G. Scappucci, M. Veldhorst, A single-hole spin qubit. *Nature* **577**(7791), 487 (2020)
9. J.R. Petta, A.C. Johnson, J.M. Taylor, E.A. Laird, A. Yacoby, M.D. Lukin, C.M. Marcus, M.P. Hanson, A.C. Gossard, Coherent manipulation of coupled electron spins in semiconductor quantum dots. *Science* **309**(5744), 2180 (2005)
10. M.J. Manfra, E.H. Hwang, S. Das Sarma, L.N. Pfeiffer, K.W. West, A.M. Sergent, Transport and percolation in a low-density high-mobility two-dimensional hole system. *Phys. Rev. Lett.* **99**(23), 236402 (2007)
11. K.C. Nowack, F.H.L. Koppens, Y.V. Nazarov, L.M.K. Vandersypen, Coherent control of a single electron spin with electric fields. *Science* **318**(5855), 1430 (2007)
12. J.M. Taylor, J.R. Petta, A.C. Johnson, A. Yacoby, C.M. Marcus, M.D. Lukin, Relaxation, dephasing, and quantum control of electron spins in double quantum dots. *Phys. Rev. B* **76**(3), 035315 (2007)
13. K.M. Itoh, H. Watanabe, Isotope engineering of silicon and diamond for quantum computing and sensing applications. *MRS Commun.* **4**(4), 143 (2014)
14. S.J. Angus, A.J. Ferguson, A.S. Dzurak, R.G. Clark, Gate-defined quantum dots in intrinsic silicon. *Nano Lett.* **7**(7), 2051 (2007)
15. D. Sabbagh, N. Thomas, J. Torres, R. Pillarisetty, P. Amin, H. George, K. Singh, A. Budrevich, M. Robinson, D. Merrill, L. Ross, J. Roberts, L. Lampert, L. Massa, S. Amitonov, J. Boter, G. Droulers, H. Eenink, M. van Hezel, D. Donelson, M. Veldhorst, L. Vandersypen, J. Clarke, G. Scappucci, Quantum transport properties of industrial $^{28}Si/^{28}SiO_2$. *Phys. Rev. Appl.* **12**, 014013 (2019)
16. V. Mazzocchi, P. Sennikov, A. Bulanov, M. Churbanov, B. Bertrand, L. Hutin, J. Barnes, M. Drozdov, J. Hartmann, M. Sanquer, 99.992% ^{28}Si CVD-grown epilayer on 300 mm substrates for large scale integration of silicon spin qubits. *J. Cryst. Growth* **509**, 1 (2019)
17. A. Zwerver, T. Krähenmann, T. Watson, L. Lampert, H. George, R. Pillarisetty, S. Bojarski, P. Amin, S. Amitonov, J. Boter, R. Caudillo, D. Corras-Serrano, J.P. Dehollain, G. Droulers, E.M. Henry, R. Kotlyar, M. Lodari, F. Luthi, D.J. Michalak, B.K. Mueller, S. Neyens, J. Roberts, N. Samkharadze, G. Zheng, O.K. Zietz, G. Scappucci, M. Veldhorst, L.M.K. Vandersypen, J.S. Clarke, Qubits made by advanced semiconductor manufacturing. Preprint, arXiv:abs/2101.12650 (2021)
18. C. Auth, A. Aliyarukunju, M. Asoro, D. Bergstrom, V. Bhagwat, J. Birdsall, N. Bisnik, M. Buehler, V. Chikarmane, G. Ding, Q. Fu, H. Gomez, W. Han, D. Hanken, M. Haran, M. Hattendorf, R. Heussner, H. Hiramatsu, B. Ho, S. Jaloviar, I. Jin, S. Joshi, S. Kirby, S. Kosaraju, H. Kothari, G. Leatherman, K. Lee, J. Leib, A. Madhavan, K. Marla, H. Meyer, T. Mule, C. Parker, S. Parthasarathy, C. Pelto, L. Pipes, I. Post, M. Prince, A. Rahman, S. Rajamani, A. Saha, J.D. Santos, M. Sharma, V. Sharma, J. Shin, P. Sinha, P. Smith, M. Sprinkle, A.S. Amour, C. Staus, R. Suri, D. Towner, A. Tripathi, A. Tura, C. Ward, A. Yeoh, “A 10nm high performance and low-power CMOS technology featuring 3rd generation FinFET transistors, self-aligned quad patterning, contact over active gate and cobalt local interconnects”, presented at the IEEE International Electron Devices Meeting, San Francisco, December, 2–6, 2017, p 29.1.1
19. W.I.L. Lawrie, H.G.J. Eenink, N.W. Hendrickx, J.M. Boter, L. Petit, S.V. Amitonov, M. Lodari, B. Paquelet Wuetz, C. Volk, S.G.J. Philips, G. Droulers, N. Kalhor, F. van Riggelen, D. Brousse, A. Sammak, L.M.K. Vandersypen, G. Scappucci, M. Veldhorst, Quantum dot arrays in silicon and germanium. *Appl. Phys. Lett.* **116**(8), 080501 (2020)
20. C.H. Yang, A. Rossi, R. Ruskov, N.S. Lai, F.A. Mohiyaddin, S. Lee, C. Tahan, G. Klimeck, A. Morello, A.S. Dzurak, Spin-valley lifetimes in a silicon quantum dot with tunable valley splitting. *Nat. Commun.* **4**(1), 2069 (2013)
21. L. Petit, H.G.J. Eenink, M. Russ, W.I.L. Lawrie, N.W. Hendrickx, S.G.J. Philips, J.S. Clarke, L.M.K. Vandersypen, M. Veldhorst, Universal quantum logic in hot silicon qubits. *Nature* **580**(7803), 355 (2020)

22. X. Xue, B. Patra, J.P. van Dijk, N. Samkharadze, S. Subramanian, A. Corna, C. Jeon, F. Sheikh, E. Juarez-Hernandez, B.P. Esparza, H. Rampurawala, B. Carlton, S. Ravikumar, C. Nieva, S. Kim, H.J. Lee, A. Sammak, G. Scappucci, M. Veldhorst, F. Sebastiano, M. Babaie, S. Pellerano, E. Charbon, L.M.K. Vandersypen, CMOS-based cryogenic control of silicon quantum circuits. Nature **593**(7858), 205 (2021)
23. S. Shankar, A.M. Tyryshkin, J. He, S.A. Lyon, Spin relaxation and coherence times for electrons at the Si/SiO_2 interface. *Phys. Rev. B* **82**(19), 195323 (2010)
24. S. Rochette, M. Rudolph, A.M. Roy, M.J. Curry, G.A.T. Eyck, R.P. Manginell, J.R. Wendt, T. Pluym, S.M. Carr, D.R. Ward, M.P. Lilly, M.S. Carroll, M. Pioro-Ladrière, Quantum dots with split enhancement gate tunnel barrier control. *Appl. Phys. Lett.* **114**(8), 083101 (2019)
25. F. Schäffler, High-mobility Si and Ge structures. *Semicond. Sci. Technol.* **12**(12), 1515 (1997)
26. J. Yoneda, K. Takeda, T. Otsuka, T. Nakajima, M.R. Delbecq, G. Allison, T. Honda, T. Kodera, S. Oda, Y. Hoshi, N. Usami, K.M. Itoh, S. Tarucha, A quantum-dot spin qubit with coherence limited by charge noise and fidelity higher than 99.9%. *Nat. Nanotechnol.* **13**(2), 102 (2018)
27. B.M. Maune, M.G. Borselli, B. Huang, T.D. Ladd, P.W. Deelman, K.S. Holabird, A.A. Kiselev, I. Alvarado-Rodriguez, R.S. Ross, A.E. Schmitz, M. Sokolich, C.A. Watson, M.F. Gyure, A.T. Hunter, Coherent singlet-triplet oscillations in a silicon-based double quantum dot. *Nature* **481**(7381), 344 (2012)
28. X. Mi, T.M. Hazard, C. Payette, K. Wang, D.M. Zajac, J.V. Cady, J.R. Petta, Magnetotransport studies of mobility limiting mechanisms in undoped Si/SiGe heterostructures. *Phys. Rev. B* **92**, 35304 (2015)
29. X. Mi, J.V. Cady, D.M. Zajac, J. Stehlik, L.F. Edge, J.R. Petta, Circuit quantum electrodynamics architecture for gate-defined quantum dots in silicon. *Appl. Phys. Lett.* **110**(4), 043502 (2017)
30. B.P. Wuetz, P. Bavdaz, L. Yeoh, R. Schouten, H. van der Does, M. Tiggelman, D. Sabbagh, A. Sammak, C. Almudever, F. Sebastiano, J.S. Clarke, M. Veldhorst, G. Scappucci. Multiplexed quantum transport using commercial off-the-shelf CMOS at sub-kelvin temperatures. *npj Quantum Inf.* **6**, 43 (2020)
31. D. Zajac, T. Hazard, X. Mi, E. Nielsen, J. Petta, Scalable gate architecture for a one-dimensional array of semiconductor spin qubits. *Phys. Rev. Appl.* **6**(5), 054013 (2016)
32. T.F. Watson, S.G.J. Philips, E. Kawakami, D.R. Ward, P. Scarlino, M. Veldhorst, D.E. Savage, M.G. Lagally, M. Friesen, S.N. Coppersmith, M.A. Eriksson, L.M.K. Vandersypen, A programmable two-qubit quantum processor in silicon. *Nature* **555**(7698), 633 (2018)
33. M.G. Borselli, K. Eng, E.T. Croke, B.M. Maune, B. Huang, R.S. Ross, A.A. Kiselev, P.W. Deelman, I. Alvarado-Rodriguez, A.E. Schmitz, M. Sokolich, K.S. Holabird, T.M. Hazard, M.F. Gyure, A.T. Hunter, Pauli spin blockade in undoped Si/SiGe two-electron double quantum dots. *Appl. Phys. Lett.* **99**(6), 063109 (2011)
34. A. Hollmann, T. Struck, V. Langrock, A. Schmidbauer, F. Schauer, T. Leonhardt, K. Sawano, H. Riemann, N.V. Abrosimov, D. Bougeard, L.R. Schreiber, Large, tunable valley splitting and single-spin relaxation mechanisms in a Si/Si_xGe_{1-x} quantum dot. *Phys. Rev. Appl.* **13**(3), 034068 (2020)
35. P. Scarlino, E. Kawakami, T. Jullien, D. Ward, D. Savage, M. Lagally, M. Friesen, S. Coppersmith, M. Eriksson, L. Vandersypen, Dressed photon-orbital states in a quantum dot: Intervalley spin resonance. *Phys. Rev. B* **95**(16), 165429 (2017)
36. S.F. Neyens, R.H. Foote, B. Thorgrimsson, T.J. Knapp, T. McJunkin, L.M. Vandersypen, P. Amin, N.K. Thomas, J.S. Clarke, D.E. Savage, M.G. Lagally, M. Friesen, S.N. Coppersmith, M.A. Eriksson, The critical role of substrate disorder in valley splitting in Si quantum wells. *Appl. Phys. Lett.* **112**(24), 243107 (2018)
37. G. Scappucci, C. Kloeffel, F.A. Zwanenburg, D. Loss, M. Myronov, J.J. Zhang, S. De Franceschi, G. Katsaros, M. Veldhorst, The germanium quantum information route. *Nat. Rev. Mater.* 1 (2020)
38. A. Sammak, D. Sabbagh, N.W. Hendrickx, M. Lodari, B.P. Wuetz, A. Tosato, L. Yeoh, M. Bollani, M. Virgilio, M.A. Schubert, P. Zaumseil, G. Capellini, M. Veldhorst, G. Scappucci, Shallow and undoped germanium quantum wells: A playground for spin and hybrid quantum technology. *Adv. Funct. Mater.* **29**(14), 1807613 (2019)
39. M. Lodari, N.W. Hendrickx, W.I.L. Lawrie, T.K. Hsiao, L.M.K. Vandersypen, A. Sammak, M. Veldhorst, G. Scappucci, Low percolation density and charge noise with holes in germanium. *Mater. Quantum Technol.* **1**(1), 011002 (2021)
40. M. Lodari, A. Tosato, D. Sabbagh, M.A. Schubert, G. Capellini, A. Sammak, M. Veldhorst, G. Scappucci, Light effective hole mass in undoped Ge/SiGe quantum wells. *Phys. Rev. B* **100**(4), 041304 (2019)
41. N.W. Hendrickx, D.P. Franke, A. Sammak, M. Kouwenhoven, D. Sabbagh, L. Yeoh, R. Li, M.L.V. Tagliaferri, M. Virgilio, G. Capellini, G. Scappucci, M. Veldhorst, Gate-controlled quantum dots and superconductivity in planar germanium. *Nat. Commun.* **9**(1), 2835 (2018)
42. N.W. Hendrickx, W.I.L. Lawrie, M. Russ, F. van Riggelen, S.L. de Snoo, R.N. Schouten, A. Sammak, G. Scappucci, M. Veldhorst, A four-qubit germanium quantum processor. *Nature* **591**(7851), 580 (2021)
43. A. Bansil, H. Lin, T. Das, Colloquium: Topological band theory. *Rev. Mod. Phys.* **88**(2), 021004 (2016)
44. N.P. Armitage, E.J. Mele, A. Vishwanath, Weyl and Dirac semimetals in three-dimensional solids. *Rev. Mod. Phys.* **90**(1), 015001 (2018)
45. Y. Ando, L. Fu, Topological crystalline insulators and topological superconductors: From concepts to materials. *Ann. Rev. Condens. Matter Phys.* **6**(1), 361 (2015)
46. S.M. Frolov, S.R. Plissard, S. Nadj-Perge, L.P. Kouwenhoven, E.P. Bakkers, Quantum computing based on semiconductor nanowires. *MRS Bull.* **38**(10), 809 (2013)
47. A. Koma, Van der Waals epitaxy-a new epitaxial growth method for a highly lattice-mismatched system. *Thin Solid Films* **216**(1), 72 (1992)
48. K. Ueno, K. Saiki, T. Shimada, A. Koma, Epitaxial growth of transition metal dichalcogenides on cleaved faces of mica. *J. Vac. Sci. Technol. A* **8**(1), 68 (1990)
49. T. Ginley, Y. Wang, S. Law, Topological insulator film growth by molecular beam epitaxy: A review. *Curr. Comput. Aided Drug Des.* **6**(11), 154 (2016)
50. A. Richardella, D.M. Zhang, J.S. Lee, A. Koser, D.W. Rench, A.L. Yeats, B.B. Buckley, D.D. Awschalom, N. Samarth, Coherent heteroepitaxy of Bi_2Se_3 on GaAs (111)B. *Appl. Phys. Lett.* **97**(26), 262104 (2010)
51. X. Liu, D.J. Smith, H. Cao, Y.P. Chen, J. Fan, Y.H. Zhang, R.E. Pimpinella, M. Dobrowolska, J.K. Furdyna, Characterization of Bi_2Te_3 and Bi_2Se_3 topological insulators grown by MBE on (001) GaAs substrates. *J. Vac. Sci. Technol. B* **30**(2), 02B103 (2012)
52. X. Guo, Z.J. Xu, H.J.C. Liu, B. Zhao, X.Q. Dai, H.T. He, J.N. Wang, H.J.C. Liu, W.K. Ho, M.H. Xie, Single domain Bi_2Se_3 films grown on InP(111)A by molecular-beam epitaxy. *Appl. Phys. Lett.* **102**(15), 151604 (2013)
53. Y.S. Kim, M. Brahlek, N. Bansal, E. Edrey, G.A. Kapilevich, K. Iida, M. Tanimura, Y. Horibe, S.W. Cheong, S. Oh, Thickness-dependent bulk properties and weak antilocalization effect in topological insulator Bi_2Se_3. *Phys. Rev. B* **84**(7), 073109 (2011)
54. J. Krumrain, G. Mussler, S. Borisova, T. Stoica, L. Plucinski, C.M. Schneider, D. Grutzmacher, MBE growth optimization of topological insulator Bi_2Te_3 films. *J. Cryst. Growth* **324**(1), 115 (2011)
55. J. Kampmeier, S. Borisova, L. Plucinski, M. Luysberg, G. Mussler, D. Grutzmacher, Suppressing twin domains in molecular beam epitaxy grown Bi_2Te_3 topological insulator thin films. *Cryst. Growth Des.* **15**, 390 (2015)
56. B. Lu, G.A. Almyras, V. Gervilla, J.E. Greene, K. Sarakinos, Formation and morphological evolution of self-similar 3D nanostructures on weakly interacting substrates. *Phys. Rev. Mater.* **2**(6), 063401 (2018)
57. J. Hellerstedt, M.T. Edmonds, J.H. Chen, W.G. Cullen, C.X. Zheng, M.S. Fuhrer, Thickness and growth-condition dependence of *in-situ* mobility and carrier density of epitaxial thin-film Bi_2Se^3. *Appl. Phys. Lett.* **105**(17), 173506 (2014)
58. T. Ginley, S. Law, Growth of Bi_2Se_3 topological insulator films using a selenium cracker source. *J. Vac. Sci. Technol. B* **34**, 02L105 (2016)
59. Y. Wang, T.P. Ginley, S. Law, Growth of high-quality Bi_2Se_3 topological insulators using $(Bi_{1-x}In_x)_2Se_3$ buffer layers. *J. Vac. Sci. Technol. B* **36**, 02D101 (2018)
60. J. Moon, N. Koirala, M. Salehi, W. Zhang, W. Wu, S. Oh, Solution to the hole-doping problem and tunable quantum hall effect in Bi_2Se_3 thin films. *Nano Lett.* **18**(2), 820 (2018)
61. H.D. Lee, C. Xu, S.M. Shubeita, M. Brahlek, N. Koirala, S. Oh, T. Gustafsson, Indium and bismuth interdiffusion and its influence on the mobility in In_2Se_3/Bi_2Se_3. *Thin Solid Films* **556**, 322 (2014)
62. M. Brahlek, N. Bansal, N. Koirala, S.Y. Xu, M. Neupane, C. Liu, M.Z. Hasan, S. Oh, Topological-metal to band-insulator transition in $(Bi_{1-x}In_x)_2Se_3$ thin films. *Phys. Rev. Lett.* **109**(18), 186403 (2012)
63. V.M. Pereira, C.N. Wu, C.A. Knight, A. Choa, L.H. Tjeng, S.G. Altendorf, Interfacing topological insulators and ferrimagnets: Bi_2Te_3 and Fe_3O_4 heterostructures grown by molecular beam epitaxy. *APL Mater.* **8**(7), 071114 (2020)
64. Z. Chen, L. Zhao, K. Park, T.A. Garcia, M.C. Tamargo, L. Krusin-Elbaum, Robust topological interfaces and charge transfer in epitaxial Bi_2Se_3/II–VI semiconductor superlattices. *Nano Lett.* **15**, 6365 (2015)
65. Z. Wang, T.P. Ginley, S.V. Mambakkam, G. Chandan, Y. Zhang, C. Ni, S. Law, Plasmon coupling in topological insulator multilayers. *Phys. Rev. Mater.* **4**(11), 115202 (2020)
66. J. Zhang, C.Z. Chang, Z. Zhang, J. Wen, X. Feng, K. Li, M. Liu, K. He, L. Wang, X. Chen, Q.K. Xue, X. Ma, Y. Wang, Band structure engineering in $(Bi_{(1-x)}Sb_{(x)})_2Te_3$ ternary topological insulators. *Nat. Commun.* **2**, 574 (2011)
67. A. Hashibon, C. Elsässer, First-principles density functional theory study of native point defects in Bi_2Te_3. *Phys. Rev. B* **84**(14), 14 (2011)
68. Z. Wang, T. Lin, P. Wei, X. Liu, R. Dumas, K. Liu, J. Shi, Tuning carrier type and density in Bi_2Se_3 by Ca-doping. *Appl. Phys. Lett.* **97**(4), 042112 (2010)
69. J. Moon, Z. Huang, W. Wu, S. Oh, Pb-doped *p*-type Bi_2Se_3 thin films via interfacial engineering. *Phys. Rev. Mater.* **4**, 024203 (2020)
70. M. Li, C.Z. Chang, L. Wu, J. Tao, W. Zhao, M.H. Chan, J.S. Moodera, J. Li, Y. Zhu, Experimental verification of the van Vleck nature of long-range ferromagnetic order in the vanadium-doped three-dimensional topological insulator Sb_2Te_3. *Phys. Rev. Lett.* **114**(14), 146802 (2015)
71. P.P. Haazen, J.B. Laloë, T.J. Nummy, H.J. Swagten, P. Jarillo-Herrero, D. Heiman, J.S. Moodera, Ferromagnetism in thin-film Cr-doped topological insulator Bi_2Se_3. *Appl. Phys. Lett.* **100**(8), 2010 (2012)
72. J. Ruzicka, O. Caha, V. Holy, H. Steiner, V. Volobuiev, A. Ney, G. Bauer, T. Duchon, K. Veltruska, I. Khalakhan, V. Matolin, E.F. Schwier, H. Iwasawa, K. Shimada, G. Spingholz, Structural and electronic properties of manganese-doped Bi_2Te_3 epitaxial layers. *New J. Phys.* **17**, 013028 (2015)

73. B. Li, W. Chen, X. Guo, W. Ho, X. Dai, J. Jia, M. Xie, Strain in epitaxial high-index Bi_2Se_3(221) films grown by molecular-beam epitaxy. *Appl. Surf. Sci.* **396**, 1825 (2017)
74. T.P. Ginley, Y. Zhang, C. Ni, S. Law, Epitaxial growth of Bi_2Se_3 in the (0015) orientation on GaAs (001). *J. Vac. Sci. Technol. A* **38**(2), 023404 (2020)
75. M.S. Claro, I. Levy, A. Gangopadhyay, D.J. Smith, M.C. Tamargo, Self-assembled Bismuth Selenide (Bi_2Se_3) quantum dots grown by molecular beam epitaxy. *Sci. Rep.* **9**(1), 3370 (2019)
76. M.S. Claro, I. Levy, T.A. Garcia, A. Gangopadhyay, D.J. Smith, M.C. Tamargo, Growth habits of bismuth selenide (Bi_2Se_3) layers and nanowires over Stranski–Krastanov indium arsenide quantum dots. *Cryst. Growth Des.* **19**(12), 6989 (2019)
77. P. Tsipas, S. Fragkos, D. Tsoutsou, C. Alvarez, R. Sant, G. Renaud, H. Okuno, A. Dimoulas, Direct observation at room temperature of the orthorhombic Weyl semimetal phase in thin epitaxial $MoTe_2$. *Adv. Funct. Mater.* **28**(33), 1802084 (2018)
78. S. Tang, C. Zhang, C. Jia, H. Ryu, C. Hwang, M. Hashimoto, D. Lu, Z. Liu, T.P. Devereaux, Z.X. Shen, S.K. Mo, Electronic structure of monolayer 1T′-$MoTe_2$ grown by molecular beam epitaxy. *APL Mater.* **6**(2), 026601 (2018)
79. P. Tsipas, D. Tsoutsou, S. Fragkos, R. Sant, C. Alvarez, H. Okuno, G. Renaud, R. Alcotte, T. Baron, A. Dimoulas, Massless dirac fermions in $ZrTe_2$ semimetal grown on InAs(111) by van der Waals epitaxy. *ACS Nano* **12**(2), 1696 (2018)
80. K. Deng, M. Yan, C.P. Yu, J. Li, X. Zhou, K. Zhang, Y. Zhao, K. Miyamoto, T. Okuda, W. Duan, Y. Wu, X. Zhong, S. Zhou, Crossover from 2D metal to 3D Dirac semimetal in metallic $PtTe_2$ films with local Rashba effect. *Sci. Bull.* **64**(15), 1044 (2019)
81. M. Yan, E. Wang, X. Zhou, G. Zhang, H. Zhang, K. Zhang, W. Yao, S. Yang, S. Wu, T. Yoshikawa, K. Miyamoto, T. Okuda, Y. Wu, P. Yu, W. Duan, S. Zhou, High quality atomically thin $PtSe_2$ films grown by molecular beam epitaxy. *2D Mater.* **4**(4), 045015 (2017)
82. S. Aminalragia-Giamini, J. Marquez-Velasco, P. Tsipas, D. Tsoutsou, G. Renaud, A. Dimoulas, Molecular beam epitaxy of thin $HfTe_2$ semimetal films. *2D Mater.* **4**(1), 015001 (2017)
83. T. Schumann, M. Goyal, H. Kim, S. Stemmer, Molecular beam epitaxy of Cd_3As_2 on a III–V substrate. *APL Mater.* **4**(12), 126110 (2016)
84. Y. Nakazawa, M. Uchida, S. Nishihaya, S. Sato, A. Nakao, J. Matsuno, M. Kawasaki, Molecular beam epitaxy of three-dimensionally thick Dirac semimetal Cd_3As_2 films. *APL Mater.* **7**(7), 071109 (2019)
85. A. Bedoya-Pinto, A.K. Pandeya, D. Liu, H. Deniz, K. Chang, H. Tan, H. Han, J. Jena, I. Kostanovskiy, S.S. Parkin, Realization of epitaxial NbP and TaP Weyl semimetal thin films. *ACS Nano* **14**, 4405 (2020)
86. J. Wen, H. Guo, C.H. Yan, Z.Y. Wang, K. Chang, P. Deng, T. Zhang, Z.D. Zhang, S.H. Ji, L.L. Wang, K. He, X.C. Ma, X. Chen, Q.K. Xue, Synthesis of semimetal A_3Bi (A = Na, K) thin films by molecular beam epitaxy. *Appl. Surf. Sci.* **327**, 213 (2015)
87. Y. Zhang, Z. Liu, B. Zhou, Y. Kim, Z. Hussain, Z.X. Shen, Y. Chen, S.K. Mo, "Molecular beam epitaxial growth of a three-dimensional topological Dirac semimetal Na_3Bi. *Appl. Phys. Lett.* **105**(3), 031901 (2014)
88. D. Samal, H. Nakamura, H. Takagi, Molecular beam epitaxy of three-dimensional Dirac material Sr_3PbO. *APL Mater.* **4**(7), 076101 (2016)
89. N. Bhattarai, A.W. Forbes, R.P. Dulal, I.L. Pegg, J. Philip, Molecular beam epitaxy growth of nonmagnetic Weyl semimetal LaAlGe thin film. *MRS Commun.* **10**(2), 272 (2020)
90. S. Li, G. Gu, E. Liu, P. Cheng, B. Feng, Y. Li, L. Chen, K. Wu, Epitaxial growth and transport properties of magnetic Weyl semimetal $Co_3Sn_2S_2$ thin films. *ACS Appl. Electron. Mater.* **2**(1), 126 (2020)
91. X. Dong, M. Wang, D. Yan, X. Peng, J. Li, W. Xiao, Q. Wang, J. Han, J. Ma, Y. Shi, Y. Yao, Observation of topological edge states at the step edges on the surface of type-II Weyl semimetal $TaIrTe_4$. *ACS Nano* **13**(8), 9571 (2019)
92. G.M. Stephen, O.A. Vail, J. Lu, W.A. Beck, P.J. Taylor, A.L. Friedman, Weak antilocalization and anisotropic magnetoresistance as a probe of surface states in topological $Bi_2Te_xSe_{3-x}$ thin films. *Sci. Rep.* **10**(1), 4845 (2020)
93. R.A. Snyder, C.J. Trimble, C.C. Rong, P.A. Folkes, P.J. Taylor, J.R. Williams, Weak-link Josephson junctions made from topological crystalline insulators. *Phys. Rev. Lett.* **121**, 097701 (2018)
94. M. Tinkham, *Introduction to Superconductivity. Dover Books on Physics*, 2nd ed. (Dover Publications, Mineola, NY, 2004), vol. 1
95. P. Sessi, D. Di Sante, A. Szczerbakow, F. Glott, S. Wilfert, H. Schmidt, T. Bathon, P. Dziawa, M. Greiter, T. Neupert, G. Sangiovanni, T. Story, R. Thomale, M. Bode, Robust spin-polarized midgap states at step edges of topological crystalline insulators. *Science* **354**(6317), 1269 (2016)
96. S.J. Pauka, K. Das, R. Kalra, A. Moini, Y. Yang, M. Trainer, A. Bousquet, C. Cantaloube, N. Dick, G.C. Gardner, M.J. Manfra, D.J. Reilly, A cryogenic interface for controlling many qubits. Preprint, arXiv:abs/1912.01299 (2019)

G. Scappucci leads the development of materials for spin-based quantum computing at QuTech/TU Delft, The Netherlands. He received his MSc degree, from the Sapienza University of Rome, Italy, in 2000, and PhD degree from Roma Tre University, Italy, in 2004. Scappucci has 20 years of experience in semiconductor materials for quantum technologies. During his MSc and PhD degrees, he made state-of-the-art high-mobility Si/SiGe heterostructures and nanowire transistors. His team developed silicon and germanium heterostructures leading to landmark achievements such as spin-photon coupling in silicon, CMOS-based cryogenic control of silicon quantum circuits, and multi-qubit logic in germanium. Scappucci can be reached by email at g.scappucci@tudelft.nl.

P. J. Taylor is a research physicist in the Sensors and Electron Devices Directorate at the US Army Research Laboratory. He received his PhD degree from the University of Virginia. He received his postdoctoral appointment with the National Academy of Sciences to develop novel electro-optical devices on silicon. Prior to his current position, Taylor held a staff appointment at the Massachusetts Institute of Technology–Lincoln Laboratory where he led the development of narrow bandgap devices for thermoelectrics as well as several advanced electro-optical devices for military communications and threat reduction. Taylor can be reached by email at patrick.j.taylor36.civ@mail.mil.

J. R. Williams is currently the Alford Ward Assistant Professor of Physics in the Department of Physics at the University of Maryland. He is also a Fellow at the Joint Quantum Institute and a member of the Quantum Materials. He completed his PhD degree at Harvard University, working on creating nanoscale devices from graphene. Previously, he was the Karl van Bibber Postdoctoral Fellow in the Physics Department at Stanford University, where he studied quantum transport in topological insulators and superconductors and complex oxide materials. His current research focuses on quantum material devices. Williams can be reached by email at jrwill@umd.edu.

T. Ginley is a postdoctoral researcher at the National Institute of Standards and Technology. She earned her PhD degree from the University of Delaware and her BS degree from Juniata College. She is the recipient of the National Research Council Postdoctoral Research Associateship, the NASA Space Grant Fellowship, the first prize poster award at the American Vacuum Society Mid-Atlantic Chapter Regional Meeting, and the University of Delaware Materials Science and Engineering Outstanding Graduate Student Service Award. Her research focuses on molecular beam epitaxy to grow novel structures such as site-controlled semiconductor quantum dots. Ginley can be reached by email at theresa.ginley@nist.gov.

S. Law is an associate professor in the Department of Materials Science and Engineering at the University of Delaware, the co-director of the University of Delaware Materials Growth Facility, and an associate editor for the Journal of Vacuum Science and Technology. She earned her PhD degree from the University of Illinois at Urbana-Champaign and BS degree from Iowa State University. Law's research uses molecular beam epitaxy to grow new materials and heterostructures such as heavily doped semiconductors, topological insulators, and other layered chalcogenide-based materials. Law's current research focuses on investigating alternative qubit materials and creating layered heterostructures for infrared and terahertz photonics. She is the recipient of the Presidential Early Career Award for Scientists and Engineers, a US Department of Energy Early Carrer Award, the International Conference on Molecular Beam Epitaxy Young Investigator Award, the American Vacuum Society Peter Mark Memorial Award, and the North American Molecular Beam Epitaxy Young Investigator Award. Law can be reached by email at slaw@udel.edu.